

# Granzyme A expression reveals distinct cytolytic CTL subsets following influenza A virus infection

Jessica M. Moffat<sup>1</sup>, Thomas Gebhardt<sup>1</sup>, Peter C. Doherty<sup>1,2</sup>,  
Stephen J. Turner<sup>1</sup> and Justine D. Mintern<sup>1</sup>

<sup>1</sup> Department of Microbiology and Immunology, The University of Melbourne, Parkville, Victoria, Australia

<sup>2</sup> Department of Immunology, St. Jude Children's Research Hospital, Memphis, TN, USA

CTL mediate anti-viral immunity via targeted exocytosis of cytolytic granules containing perforin and members of the granzyme (grz) serine protease family. Here, we provide the first analysis of grzA protein expression by murine anti-viral CTL. During the progression of influenza A virus infection, CTL expressed two divergent cytolytic phenotypes: grzA<sup>-</sup>B<sup>+</sup> and grzA<sup>+</sup>B<sup>+</sup>. CTL lacked grzA expression during the initial rounds of antigen-driven division. High levels of grzA were expressed by influenza-specific CTL early post infection (day 6), particularly in tissues associated with the infected respiratory tract (bronchoalveolar lavage, lung). Following resolution of influenza infection, a small population of memory CTL expressed grzA. Interestingly, individual influenza A virus-derived epitope-specific CTL expressed different levels of grzA. The grzA expression hierarchy was determined to be K<sup>b</sup>PB1<sub>703</sub> = D<sup>b</sup>F2<sub>62</sub> = K<sup>b</sup>NS2<sub>114</sub> > D<sup>b</sup>NP<sub>366</sub> = D<sup>b</sup>PA<sub>224</sub> and inversely correlated with CTL magnitude. Therefore following influenza infection, a CTL cytolytic hierarchy was established relating to the different profiles of antigen expression and relative immunodominance. Analysis of CTL grzA expression during influenza virus immunity has enabled a more detailed insight into the cytolytic mechanisms of virus elimination.

**Key words:** Cell differentiation · Cytotoxicity · T cells · Viral

## Introduction

CD8<sup>+</sup> CTL are critical for limiting and eventual clearing of viral infection. Naïve CTL encounter virus-derived peptides, presented in the context of MHC class I glycoproteins (pMHCI) on the surface of antigen-presenting DC, within LN draining the infected tissue. Once activated naïve CTL undergo a program of proliferation and subsequent acquisition of effector function that includes expression of cytotoxic proteins and the capacity to secrete pro-inflammatory cytokines. A major pathway by which CTL clear virus infection is the targeted exocytosis of granules containing various cytolytic proteins, including the pore-forming protein perforin (pfp), and members of the granzyme (grz) serine

protease family, towards the infected cell [1]. Once delivered, pfp and grz act synergistically to initiate programmed cell death by both caspase-dependent and independent pathways [2].

The most well-characterised CTL cytolytic effector protein is grzB. Mouse grzB cleaves substrate proteins resulting in classical apoptotic death characterised by mitochondrial depolarisation, nuclear fragmentation, and DNase activation. Naïve CTL express grzB early after antigen encounter [3, 4], with both increased mRNA and protein expression correlating with progressive cell division [5–7]. Although effector CTL express abundant levels of grzB protein at the peak of the response [8], this is largely turned off as the CTL population contracts into memory [9–12]. Given its important role in CTL-mediated killing, many viruses have evolved strategies that target and disable grzB function [13]. In the face of such inhibitors, presumably other grz family members must be utilised if CTL killing is to proceed upon virus infection.

**Correspondence:** Dr. Stephen J. Turner  
e-mail: sjturn@unimelb.edu.au

Similar to grzB, grzA is a well-characterised member of the grz protease family although it mediates cell death via distinct pathways [14]. Although the role of grzA in CTL killing is less well defined than that of grzB, grzA-deficient mice demonstrate increased susceptibility to ectromelia virus infection [15], highlighting grzA participation in immunity to natural host–pathogen interactions. Recently, an intriguing function for grzA in eliciting inflammation has been described. Metkar *et al.* provide evidence that both mouse and human grzA stimulate monocytic cells to secrete proinflammatory cytokines [16]. The study of grzA may therefore yield insights into the broader biological roles of the grz family.

Single virus-specific CTL display distinct and heterogeneous patterns of pfp and grz mRNA transcripts after *in vitro* and *in vivo* activation [8, 12, 17, 18]. Heterogeneous patterns of effector mRNA expression are thought to reflect independent regulatory mechanisms. This was supported by a recent analysis showing that grzB mRNA is expressed earlier than grzA message [7]. Although grzA transcription has been studied extensively, grzA protein expression by murine CTL remains to be described. Studies of human virus-specific CTL have demonstrated significant grzA expression [19–21]; however, the limited availability of reagents, particularly for murine grz, has restricted this type of analysis for the different cytolytic proteins. Therefore, it is currently unknown whether the transcriptional heterogeneity characteristic of virus-specific CTL is indeed reflected in distinct expression profiles for the corresponding cytolytic proteins. Using a recently described anti-murine grzA antibody [22], we exam-

ined grzA and grzB co-expression within murine influenza A virus-specific CTL. Interestingly, there is considerable heterogeneity that can be related to the various pMHC complexes that drive influenza A virus CTL clonal expansion and determine response magnitude.

## Results

### Detection of grzA expression by CTL following influenza A virus infection

To determine the extent of grzA and grzB co-expression within influenza-specific CTL, C57BL/6 (B6) mice were infected i.n. with  $1 \times 10^4$  PFU A/HKx31 (X31) and lymphocytes isolated 10 days after infection. This time point represents the peak of CD8<sup>+</sup> T-cell magnitude during primary X31 infection. GrzA expression by CD8<sup>+</sup> T cells was not detected in uninfected hosts (data not shown). GrzA expression, relative to cells stained with an isotype control antibody, was detected within both splenic CD8<sup>+</sup> and CD8<sup>-</sup> populations (Fig. 1A). The CD8<sup>-</sup>grzA<sup>+</sup> population is presumably NK cells [22]. Interestingly, CD8<sup>+</sup>grzA<sup>+</sup> CTL were always a subset of CD8<sup>+</sup>grzB<sup>+</sup> influenza A virus-specific CTL (Fig. 1B). In an effort to distinguish grzA<sup>+</sup> from grzA<sup>-</sup> CTL based on the expression of other activation molecules, a panel of surface molecules associated with CTL activation; CD62L, CD69, CD25, CD27, CD127, CD43, killer cell lectin-like receptor G-1 (KLRG-1), was examined for co-expression with either grzB or grzA. Indicative of an effector phenotype, the

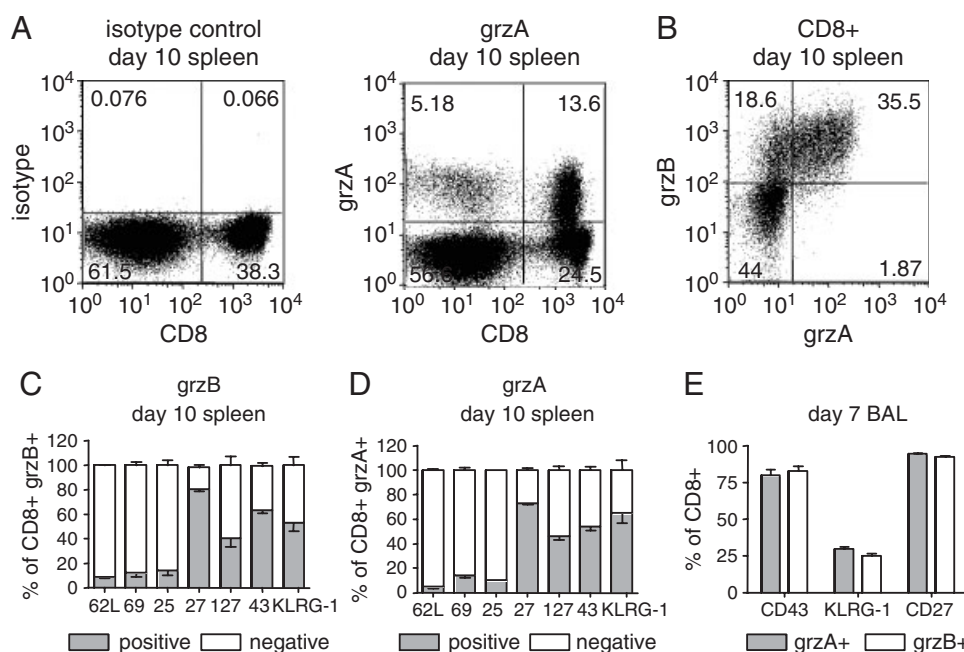


**Figure 1.** Detection of grzA expression by CTL following influenza A virus infection. B6 mice were infected i.n. with  $1 \times 10^4$  PFU X31 influenza A virus. (A) The spleen was harvested 10 days following infection and the expression of grzA versus CD8 determined for total spleen cells by staining with an isotype control antibody or anti-grz A antibody. (B) grzA versus grz B determined for CD8<sup>+</sup> T cells. The expression of CD62L (62L), CD69 (69), CD25 (25), CD27 (27), CD127 (127), CD43 (43), and KLRG-1 was examined for (C) grzB or (D) grzA-expressing CD8<sup>+</sup> cells. (E) BAL was harvested at day 7 following X31 infection and the percentage of grzA<sup>+</sup> or grzB<sup>+</sup> CD8<sup>+</sup> T cells that co-expressed CD43, KLRG-1 or CD27 was determined. Data show mean  $\pm$  SEM ( $n = 3$ –6 mice).

majority of grzA<sup>+</sup> and/or grzB<sup>+</sup> CTL, in the spleen at day 10, displayed a CD62L<sup>low</sup>, CD69<sup>low</sup>, CD25<sup>low</sup>, CD27<sup>high</sup>, CD127<sup>low to high</sup>, CD43<sup>low to high</sup>, KLRG-1<sup>low to high</sup> phenotype (Fig. 1C and D). No major difference between the grzA<sup>+</sup> and grzB<sup>+</sup> CTL was observed. This was also the case at early (day 7) time points in the respiratory tract (Fig. 1E).

### Differential expression of grzA versus grzB during CD8<sup>+</sup> T-cell division

GrzA expression during initial rounds of CD8<sup>+</sup> T-cell division was examined. Previously, grzB expression has been associated with increased CD8<sup>+</sup> T-cell division [5–7]. To enable the detection of antigen-specific CD8<sup>+</sup> T-cell division, CFSE-labelled CD8<sup>+</sup> H-2K<sup>b</sup> + OVA amino acid residues 257–264 (K<sup>b</sup>OVA<sub>257</sub>)-specific T cells (OT-I) were adoptively transferred into mice that had been i.n. infected with  $1 \times 10^4$  PFU X31-OVA 3 days previously. In these mice, transferred OT-I will divide in response to the abundantly expressed K<sup>b</sup>OVA<sub>257</sub> presented in the mediastinal LN (MLN) that drains the infected lung [7]. Prior to transfer, OT-I did not express grzA or grzB (Fig. 2A). Seven days following X31-OVA infection, transferred OT-I expressed abundant levels of grzA and grzB (Fig. 2B). For division analysis, MLN were harvested ~64 h following OT-I transfer and the expression of grzA and/or grzB was determined. In accordance with previous reports [5–7], grzB expression was detected in dividing OT-I that had undergone multiple (>3) divisions (Fig. 2C).

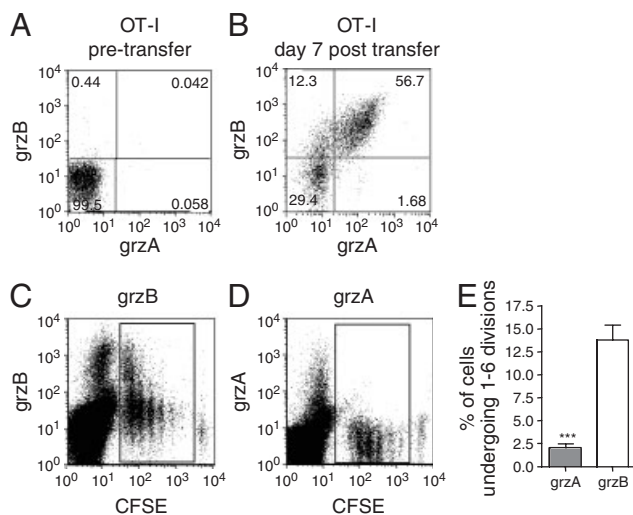


**Figure 2.** Differential expression of grzA versus grzB during CD8<sup>+</sup> T cell division. B6 mice were infected i.n. with  $1 \times 10^4$  PFU X31-OVA. A total of  $2 \times 10^6$  CFSE-labelled OT-I were transferred into X31-OVA infected mice 3 days following infection. Grz expression by OT-I was determined (A) prior to transfer and (B) 7 days following X31-OVA infection. For division analysis, MLN were harvested at 64 h following CFSE-OT-I transfer and the expression of grzB or grzA determined. Representative dot plots of CFSE expression versus (C) grzB or (D) grzA. (E) Graph summarising expression of grzB or grzA by dividing OT-I. Grz expression was determined for cells undergoing 1–6 divisions based on CFSE dilution (gate displayed on dot plots). Data show mean  $\pm$  SEM ( $n = 7$  mice). The data is pooled from two independent infections. \*\*\* $p < 0.001$  (Mann–Whitney U test).

Surprisingly, grzA expression was not observed within OT-I that had undergone up to six divisions and was detected only in CFSE-negative cells (host cells) (Fig. 2D). Overall, the proportion of grzA<sup>+</sup> OT-I was significantly ( $p < 0.001$ ) lower than the proportion of grzB<sup>+</sup> OT-I for cells that had undergone 1–6 divisions (Fig. 2E).

### Kinetics and localisation of grzA and grzB expressing CTL

To gain further insight into the regulation of grzA by influenza A virus-specific CTL, the kinetics of grzA (and grzB) expression was determined at early (day 6), peak (days 8–9), and late (days 14–17) time points after infection. CTL were harvested from all sites associated with pulmonary infection: MLN, bronchoalveolar lavage (BAL), and lung. Lymphocytes were stained with a panel of tetrameric D<sup>b</sup> or K<sup>b</sup> MHC class I molecules loaded with peptides representing the major influenza-derived epitopes presented in the B6 model of infection: H-2D<sup>b</sup> + nucleoprotein amino acid residues 366–374 (D<sup>b</sup>NP<sub>366</sub>), H-2D<sup>b</sup> + acid polymerase amino acids 224–233 (D<sup>b</sup>PA<sub>224</sub>), H-2K<sup>b</sup> + polymerase B amino acids 703–711 (K<sup>b</sup>PB1<sub>703</sub>), H-2D<sup>b</sup> + alternative reading frame polymerase B amino acids 62–70 (D<sup>b</sup>F<sub>262</sub>) and H-2K<sup>b</sup> + non-structural protein 2 NS2<sub>114–121</sub> (D<sup>b</sup>NS<sub>2114</sub>). At early, peak, and late time points two major cytolytic subsets of influenza A virus-specific CTL (grzA<sup>−</sup>B<sup>+</sup> and grzA<sup>+</sup>B<sup>+</sup>) were detected and the proportion of grzA<sup>−</sup>B<sup>+</sup> versus grzA<sup>+</sup>B<sup>+</sup> CTL was compared at each time point and across the different organs. At the early time point (Fig. 3A), the proportion of grzA<sup>−</sup>B<sup>+</sup> CTL, compared with grzA<sup>+</sup>B<sup>+</sup> CTL, was significantly increased in the BAL ( $p < 0.01$ ) and lung ( $p < 0.01$ ), but not in the MLN where the two subsets were equivalently represented. This distribution was unique to the early time point as at the peak of the CD8<sup>+</sup> T-cell response, a significant increase in the proportion of grzA<sup>−</sup>B<sup>+</sup> CTL, compared with grzA<sup>+</sup>B<sup>+</sup> CTL, was detected in the MLN ( $p < 0.05$ ), BAL ( $p < 0.01$ ), and lung ( $p < 0.05$ ) (Fig. 3B). This was also the case at the late time point ( $p < 0.01$ ) (Fig. 3C). In summary, the data illustrate enrichment for grzA<sup>−</sup>B<sup>+</sup> CTL early in the infected respiratory tract, while at the peak and late time points, this is reversed, with grzA<sup>−</sup>B<sup>+</sup> CTL being the dominant cytolytic CTL subset.

### Characterisation of memory CTL expressing grzA and grzB

Following resolution of influenza infection, CTL contract into a memory pool that is maintained in both the lymphoid and peripheral tissue. Although previous reports have demonstrated that influenza-specific memory CTL express little grzB protein [8], this has not been determined for grzA. The expression of grzA and/or grzB by splenic or lung-resident influenza A virus-specific memory CTL was assessed. The proportion of memory CTL that expressed grzB ( $p < 0.01$ ) was significantly increased in the lung compared with the spleen. In contrast, grzA-expressing memory CTL were represented equivalently in both the spleen and the lung (Fig. 4A). Effector memory CTL are associated with

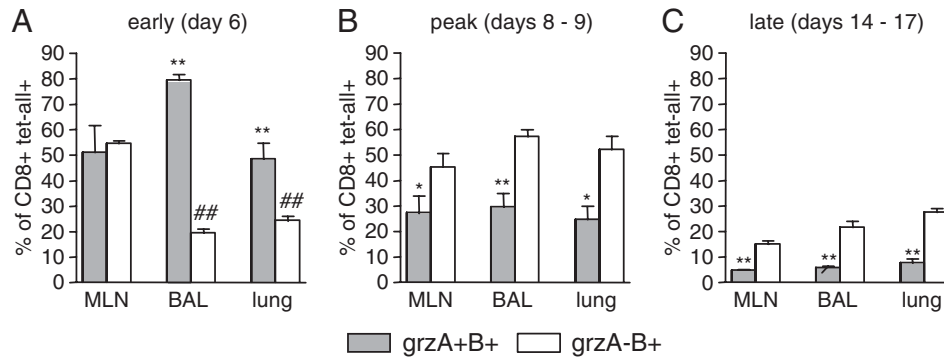


**Figure 3.** Kinetics and localisation of grzA and grzB expressing CTL. MLN, BAL, or lung were harvested at (A) early (day 6), (B) peak (days 8–9), or (C) late (days 14–17) time points following i.n. infection with  $1 \times 10^4$  PFU X31 and the expression of grzA and grzB by  $CD8^+ K^bD^b$  influenza $^+$  (tet-all $^+$ ) cells examined by flow cytometry. Graphs display the percentage of grzA $^+B^+$  (grey bars) versus grzA $^-B^+$  (white bars) within  $CD8^+ K^bD^b$  influenza $^+$  (tet-all $^+$ ) cells in each organ. The bars represent mean  $\pm$  SEM, where  $n = 6$  for early,  $n = 8$  for peak and  $n = 5$  for late time points. The data are pooled from 2–3 independent infections. \*\* $p < 0.01$ , \* $p < 0.05$  for differences between grzA $^+B^+$  and grzA $^-B^+$  CTL.  $^{##}p < 0.01$  for differences between MLN versus BAL or lung (Mann–Whitney  $U$  test).

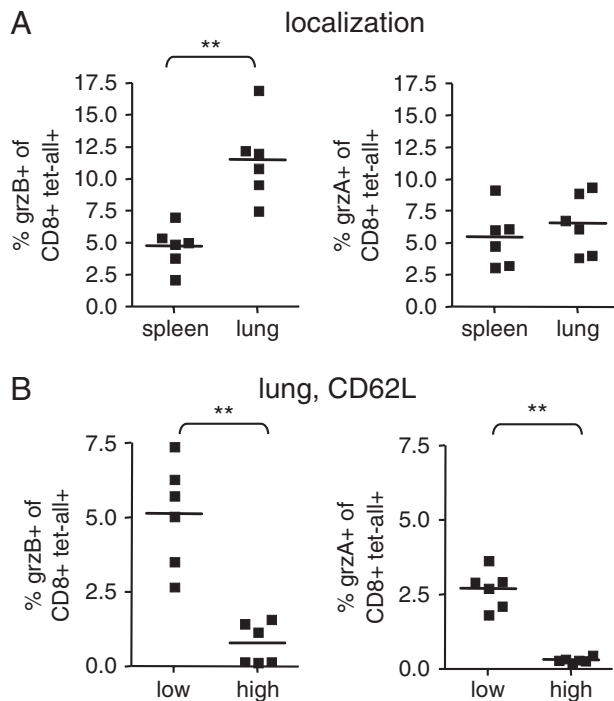


**Figure 4.** Characterisation of memory CTL expressing grzA and grzB. B6 mice were infected i.n. with  $1 \times 10^4$  PFU X31. Spleen and lung were harvested 30–60 days following infection and the expression of grzA and/or grzB by  $CD8^+ K^bD^b$  influenza $^+$  (tet-all $^+$ ) cells examined. (A) The proportion of grzB $^+$  or grzA $^+$   $CD8^+ K^bD^b$  influenza $^+$  (tet-all $^+$ ) cells present in the spleen or lung. (B) The proportion of CD62L $^{low}$  (low) or CD62L $^{high}$  (high)  $CD8^+ K^bD^b$  influenza $^+$  cells that express grzA or grzB in the lung. Each square represents an individual mouse and the bar indicates the mean, pooled from two independent experiments. \*\* $p < 0.01$  (Mann–Whitney  $U$  test).

cytotoxic function and display a CD62L $^{low}$  phenotype [23]. In the lung (Fig. 4B) and spleen (data not shown), both grzB $^+$  and grzA $^+$  memory CTL expressed a CD62L $^{low}$  phenotype.

### The expression of grzA varies for CTL specific for different virus-derived epitopes

So far, we have examined the expression of grzA and/or grzB by a pooled population of influenza A virus-specific CTL with varied pMHC I epitope specificities. To analyse the response in more detail, we determined grzA and/or grzB expression by the distinct influenza-epitope-specific CTL. In the BAL 10 days after primary infection, a comparable level of grzB was observed for individual influenza-specific CTL (Fig. 5A). This was also the case in the spleen (data not shown). In contrast, grzA expression varied significantly between individual CTL of differing specificities (Fig. 5B and C). A significantly lower proportion of D $^b$ NP $_{366}$ - and D $^b$ PA $_{224}$ -specific CTL expressed grzA compared with K $^b$ PB1 $_{703}$  ( $p < 0.01$ ), D $^b$ F2 $_{62}$  ( $p < 0.05$ ), and K $^b$ NS2 $_{114}$ -specific CTL ( $p < 0.05$ ) (Fig. 5B). The increased proportion of grzA $^+B^+$  CTL within the K $^b$ PB1 $_{703}$ - ( $p < 0.01$ ), D $^b$ F2 $_{62}$ - ( $p < 0.05$ ), and K $^b$ NS2 $_{114}$ -specific CTL ( $p < 0.05$ ), relative to D $^b$ NP $_{366}$ - and D $^b$ PA $_{224}$ -specific CTL, was also detected in the spleen (Fig. 5C). Therefore, the cytolytic hierarchy of the individual influenza A virus-specific populations was K $^b$ PB1 $_{703}$  = D $^b$ F2 $_{62}$  = K $^b$ NS2 $_{114}$  > D $^b$ NP $_{366}$  = D $^b$ PA $_{224}$ . The proportion of grzA $^+B^+$  CTL within the K $^b$ PB1 $_{703}$ -specific CTL population was also significantly ( $p < 0.05$ ) increased relative to D $^b$ NP $_{366}$ -specific CTL at a later (day 14–16) time point (Fig. 5D). To further probe the distinct expression of grzA by different epitope-specific CTL, we examined responses following X31-OVA infection. K $^b$ OVA $_{257}$ -specific CTL displayed a similar proportion of grzA $^+B^+$  CTL to K $^b$ PB1 $_{703}$ -specific CTL and was significantly ( $p < 0.001$ ) increased relative to D $^b$ NP $_{366}$ -specific CTL (Fig. 5E). Therefore, within a responding antiviral CTL population, CTL specific for different virus-derived epitopes express different levels of grzA.

Expression of grzA by CTL specific for a given epitope, but presented in different infectious contexts, was also examined. In response to HSV-1, the majority of CTL are specific for H-2K $^b$  + glycoprotein B amino acid residues 498–505 (K $^b$ gB $_{498}$ ) [24]. By utilising a recombinant WSN-gB influenza A virus, the impact of

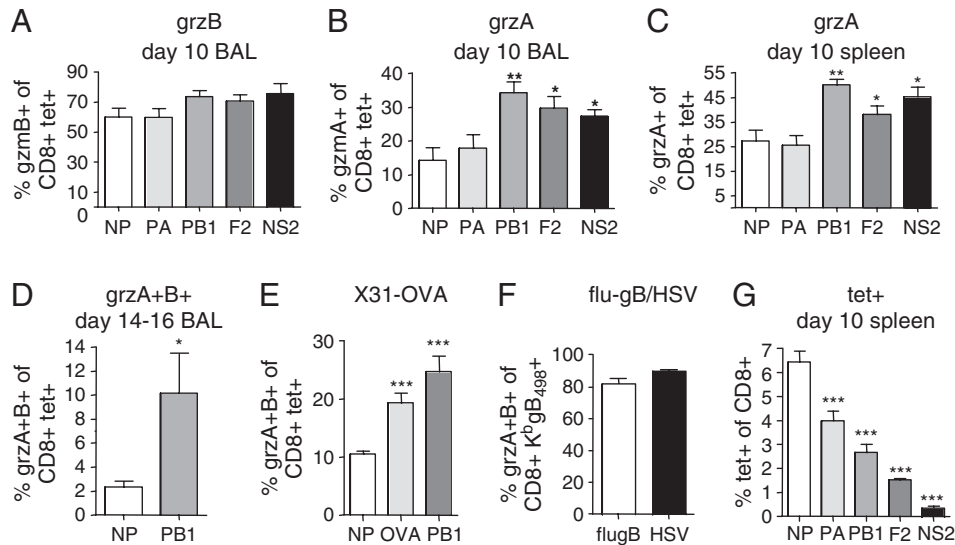


**Figure 5.** The expression of grzA varies for CTL specific for different virus-derived epitopes. B6 mice were infected i.n. with  $1 \times 10^4$  PFU X31. At 10 days following infection, the expression of (A) grzB (grzA<sup>-</sup>B<sup>+</sup> or grzA<sup>+</sup>B<sup>+</sup>) (B) or grzA (grzA<sup>+</sup>B<sup>+</sup>) by D<sup>b</sup>NP<sub>366</sub> (NP)-, D<sup>b</sup>PA<sub>224</sub> (PA)-, K<sup>b</sup>PB1<sub>703</sub> (PB1)-, D<sup>b</sup>F2<sub>62</sub> (F2)-, and K<sup>b</sup>NS2<sub>114</sub> (NS2)-specific CTL (tet<sup>+</sup>) was examined in cells present in the BAL (A and B) or (C) spleen by flow cytometry. (D) Expression of grzA and grzB by D<sup>b</sup>NP<sub>366</sub> (NP)- or K<sup>b</sup>PB1<sub>703</sub> (PB1)-specific CTL present in the BAL at days 14–16 following infection with  $1 \times 10^4$  PFU X31. (E) B6 mice were infected i.n. with X31-OVA and the BAL examined 10 days following infection for grzA and grzB expression by D<sup>b</sup>NP<sub>366</sub> (NP), K<sup>b</sup>OVA<sub>257</sub> (OVA), K<sup>b</sup>PB1<sub>703</sub> (PB1)-specific CTL. (F) Expression of grzA and grzB by K<sup>b</sup>gB<sub>498</sub>-specific CTL present in the spleen following infection i.n. with flu-gB or flank infection with  $1 \times 10^6$  PFU HSV-1. (G) B6 mice were infected i.n. with  $1 \times 10^4$  X31. At 10 days the percentage of D<sup>b</sup>NP<sub>366</sub> (NP), D<sup>b</sup>PA<sub>224</sub> (PA), K<sup>b</sup>PB1<sub>703</sub> (PB1), D<sup>b</sup>F2<sub>62</sub> (F2), and K<sup>b</sup>NS2<sub>114</sub> (NS2)-specific CTL in the CD8<sup>+</sup> T-cell population was determined for cells in the spleen. Data show mean  $\pm$  SEM, pooled from 2–3 independent experiments ( $n = 5$ –10 mice). \*\*\* $p < 0.001$ , \*\* $p < 0.01$ , \* $p < 0.05$  for differences between specific epitope and NP<sub>366</sub> (Mann–Whitney  $U$  test).

different viral infections (HSV-1 *versus* influenza A virus) on grzA expression by K<sup>b</sup>gB<sub>498</sub>-specific CTL can be determined. Both HSV-1 and influenza A virus infection induced similar levels of grzA<sup>+</sup>B<sup>+</sup> expression within K<sup>b</sup>gB<sub>498</sub>-specific CTL (Fig. 5F). Therefore, distinct epitope-specific CTL display unique cytolytic profiles, independent of the infectious viral context. Finally, to determine if there was a correlation between grzA expression and immunodominance hierarchies, the magnitude of each epitope-specific CTL population was determined. The hierarchy of CTL magnitude was D<sup>b</sup>NP<sub>366</sub> > D<sup>b</sup>PA<sub>224</sub> > K<sup>b</sup>PB1<sub>703</sub> > D<sup>b</sup>F2<sub>62</sub> > K<sup>b</sup>NS2<sub>114</sub> in the spleen (Fig. 5G). Interestingly, this inversely correlated with the observed grzA expression hierarchy, with the exception that D<sup>b</sup>PA<sub>224</sub>-specific CTL do not express higher grzA than D<sup>b</sup>NP<sub>366</sub>-specific CTL. The larger the CTL population, the less likely it is to express high levels of grzA.

## Discussion

Here, we describe the expression of grzA by cytolytic CTL populations with the progression of influenza A virus infection. At early time points, grzA<sup>+</sup>B<sup>+</sup> CTL were the dominant population, particularly in the infected respiratory tract (BAL, lung). Conversely, at the peak of CTL magnitude and at later time points, CTL expressing only grzB represented the major cytolytic CTL population. These data support the notion that the different grz family members are regulated independently. Previous analysis of effector mRNA expression has demonstrated that there is heterogeneity of grz/pfp expression within virus-specific

CTL, with little evidence of effector mRNA co-expression [7, 8, 12, 25]. To date, this heterogeneity has not been examined at the protein level for murine virus-specific CTL. Independent grz regulation is observed for resting murine NK cells that contain abundant grzA protein but little grzB [22]. Our analysis demonstrated that grzA was expressed only together with grzB in all of the virus-specific CTL populations examined. Co-expression of grzA with grzB was also the case for *in vitro* activated human PBMC [21]. Conversely, for human CTL induced by smallpox vaccination, grzB<sup>+</sup> CTL were a subset of the grzA<sup>+</sup> population [20]. The disparity in grz expression between human and murine CTL may be indicative of interspecies differences exhibited by the grz proteins. Human and murine grzA are structurally divergent [26] and as such possess different cytotoxic capacities [27]. This is also the case for grzB, where the human and murine proteins display dissimilar cytotoxic function, modes of cell death and unique substrate specificities [27, 28]. The specialised functions of human *versus* murine grz likely occur due to the unique immune evolutionary pressures faced by each species. However, murine grzA protein expression is clearly tightly regulated and its expression by anti-viral CTL is elicited by signals distinct to those required to elicit grzB expression alone.

Interestingly, we observed that different influenza A virus-specific CTL contained varied levels of grzA protein. Thus, CTL display a unique cytolytic hierarchy that is reflective of their epitope-determined differentiation status. A comparable situation is observed for CTL cytokine production during influenza A virus infection [29]. Determining why some CTL express high levels of

grzA, while others do not, may shed insight into the role of grzA during virus infection. Increased grzA expression by a subset of influenza epitope-specific CTL did not correlate with reported TCR avidities or reflect a distinct effector cytokine pattern [29–31]. For example, although D<sup>b</sup>NP<sub>366</sub>- and D<sup>b</sup>PA<sub>224</sub>-specific CTL display significantly different cytokine patterns and TCR avidity [29, 30], expression of grzA was similar. In contrast, although D<sup>b</sup>PA<sub>224</sub>- and K<sup>b</sup>PB1<sub>703</sub>-specific CTL display similar cytokine profiles [29, 31], grzA was differentially expressed. Instead, here we observed an inverse correlation between grzA expression and the magnitude of the epitope-specific response. Co-expression of more than one grz family member has been shown to increase cytotoxic activity *in vitro* [32]. This would imply that CTL expressing higher levels of grzA are more potent killers. Therefore, the inverse correlation between magnitude and grzA could imply that the smaller “subdominant” CTL sets compensate for their diminished prevalence and elicit more potent cytolytic killing *via* co-expression of grzA and grzB. Extended activation may be required for grzA expression, given that recently activated CTL did not express grzA within the first seven rounds of division detected by CFSE dilution. The higher expression of grzA by selected CTL subsets may therefore indicate differences in the duration and timing of antigen presentation throughout the course of infection. Finally, an intriguing possibility for the varied grzA levels is that grzA expression reflects the capacity of some CTL subsets to engage in effector functions other than cytotoxicity. A very interesting recent report describes the ability of grzA to induce proinflammatory cytokine production [16]. Inflammatory cascades can have a deleterious impact during influenza infection [33] and as such CTL subsets with higher grzA levels may contribute to immunopathology rather than protection. These possibilities remain to be investigated.

In conclusion, we have provided an in-depth assessment of grzA expression during anti-viral immunity. The present analysis shows, for the first time in a murine system, that grzA and grzB protein expression profiles are divergent during the course of the virus-specific CTL response. This is related to the different profiles of pMHC I expression and relative CTL immunodominance. Of interest would be to extend this type of analysis to other grz. For example, grzK is implicated in anti-viral CTL immunity based on transcriptional data [7, 8, 12, 34]. Investigation of cytolytic protein expression by CTL will enable in-depth understanding of these proteins that are critical for viral clearance.

## Materials and methods

### Mice and viral infections

B6 mice were bred and housed in the Department of Microbiology and Immunology animal facility at The University of Melbourne. Naïve mice (6–8 wk) were *i.n.* infected with  $1 \times 10^4$  PFU of X31 or X31-OVA [35] or WSN-gB influenza A virus. For HSV-1 infection, mice were inoculated with  $1 \times 10^6$  PFU HSV-1

(KOS strain) in a region of scarified flank skin. All experiments were performed in compliance with The University of Melbourne Animal Experimental Ethics Committee guidelines.

### Tissue sampling and single-cell preparations

MLN, spleen, BAL, and lungs were harvested from infected mice. Spleen cell suspensions were prepared using a 40–70 µm nylon cell strainer (BD Falcon, MA, USA), followed by treatment with red cell lysis buffer (0.14 M NH<sub>4</sub>Cl, 0.017 M Tris). MLN cell suspensions were prepared by tissue dissociation using forceps. BAL samples were treated with red cell lysis buffer. Lung tissue was digested in the presence of 2 mg/mL of collagenase A (Roche, IN) at 37°C for 30 min, followed by dissociation through a 40–70 µm nylon sieve (BD Falcon) and treatment with red cell lysis buffer.

### Tetramer, antibody, and intracellular staining

Single-cell suspensions were stained with fluorescent-conjugated MHC class I tetramers for 1 h at room temperature in PBS containing 1% bovine albumin (Invitrogen) and 0.02% sodium azide (Sigma Aldrich). Tetramers used were D<sup>b</sup>NP<sub>366</sub>, D<sup>b</sup>PA<sub>224</sub>, K<sup>b</sup>PB1<sub>703</sub>, D<sup>b</sup>F2<sub>62</sub>, and K<sup>b</sup>NS2<sub>114</sub> for influenza A virus infection, K<sup>b</sup>OVA<sub>257</sub> for X31-OVA infection, and K<sup>b</sup>gB<sub>498</sub> for HSV-1 infection. Surface staining was performed with fluorescently conjugated anti-mouse CD8 (Clone 53–6.7: BD Biosciences), CD62L (Clone MEL-14: BD Biosciences), CD69 (Clone HI.2F3: Biolegend), CD25 (Clone PC61: BD Biosciences), CD27 (Clone LG.3A10: BD Biosciences), CD127 (Clone SB/199: BD Biosciences), CD43 (Clone 1B11: Biolegend), or KLRG-1 (Clone 2F1: BD Biosciences). Samples were fixed and permeabilised using the BD Cytofix/Cytoperm kit (BD Biosciences). Intracellular grz staining was performed using anti-mouse grzA-PE/FITC (Clone 3G8.5: Santa Cruz Biotechnology) or isotype control; normal mouse IgG2b-FITC (Clone SC-2857: Santa Cruz Biotechnology) and anti-human grzB-APC (Clone MHGB05: Caltag) for 30 min on ice. Data was acquired on a FACSCaliber (BD Immunocytometry Systems) and analysed using Flow Jo software.

### CFSE-labelling and adoptive transfer

LN were harvested from OT-I TCR transgenic mice [36] and single-cell suspensions were prepared. CFSE labelling was performed by incubating  $10^7$  cells/mL in PBS containing 1% bovine albumin (Invitrogen), with 5 µM of CFSE (Invitrogen) at 37°C for 10 min. Mice were *i.v.* injected with  $2 \times 10^6$  CFSE labelled CD8<sup>+</sup> TCR transgenic T cells. At approximately 64 h post transfer, MLN were harvested and analysed by flow cytometry.

### Statistical analysis

All graphing and statistical analyses were performed using the Prism graphing program. *p*-Values were calculated using a non-parametric Mann–Whitney *T* test.

**Acknowledgements:** J.D.M. was supported by an NHMRC (Australia) Grant (no. 508905) and The University of Melbourne C.R. Roper Fellowship. P.C.D. was supported by an NHMRC (Australia) Burnet Grant. S.J.T. was supported by a Pfizer Senior Research Fellowship.

**Conflict of interest:** The authors declare no financial or commercial conflict of interest.

## References

- 1 Trapani, J. A. and Smyth, M. J., Functional significance of the perforin/granzyme cell death pathway. *Nat. Rev. Immunol.* 2002. **2**: 735–747.
- 2 Chowdhury, D. and Lieberman, J., Death by a thousand cuts: granzyme pathways of programmed cell death. *Annu. Rev. Immunol.* 2008. **26**: 389–420.
- 3 Chiu, C., Heaps, A. G., Cerundolo, V., McMichael, A. J., Bangham, C. R. and Callan, M. F., Early acquisition of cytolytic function and transcriptional changes in a primary CD8<sup>+</sup> T-cell response *in vivo*. *Blood* 2007. **109**: 1086–1094.
- 4 Lawrence, C. W., Ream, R. M. and Braciale, T. J., Frequency, specificity, and sites of expansion of CD8<sup>+</sup> T cells during primary pulmonary influenza virus infection. *J. Immunol.* 2005. **174**: 5332–5340.
- 5 Meng, Y., Harlin, H., O'Keefe, J. P. and Gajewski, T. F., Induction of cytotoxic granules in human memory CD8<sup>+</sup> T cell subsets requires cell cycle progression. *J. Immunol.* 2006. **177**: 1981–1987.
- 6 Lawrence, C. W. and Braciale, T. J., Activation, differentiation, and migration of naive virus-specific CD8<sup>+</sup> T cells during pulmonary influenza virus infection. *J. Immunol.* 2004. **173**: 1209–1218.
- 7 Jenkins, M. R., Mintern, J., La Gruta, N. L., Kedzierska, K., Doherty, P. C. and Turner, S. J., Cell cycle-related acquisition of cytotoxic mediators defines the progressive differentiation to effector status for virus-specific CD8<sup>+</sup> T cells. *J. Immunol.* 2008. **181**: 3818–3822.
- 8 Jenkins, M. R., Kedzierska, K., Doherty, P. C. and Turner, S. J., Heterogeneity of effector phenotype for acute phase and memory influenza A virus-specific CTL. *J. Immunol.* 2007. **179**: 64–70.
- 9 Kaech, S. M., Hemby, S., Kersh, E. and Ahmed, R., Molecular and functional profiling of memory CD8 T cell differentiation. *Cell* 2002. **111**: 837–851.
- 10 Wherry, E. J., Teichgraber, V., Becker, T. C., Masopust, D., Kaech, S. M., Antia, R., von Andrian, U. H. and Ahmed, R., Lineage relationship and protective immunity of memory CD8 T cell subsets. *Nat. Immunol.* 2003. **4**: 225–234.
- 11 Byers, A. M., Kemball, C. C., Moser, J. M. and Lukacher, A. E., Cutting edge: rapid *in vivo* CTL activity by polyoma virus-specific effector and memory CD8<sup>+</sup> T cells. *J. Immunol.* 2003. **171**: 17–21.
- 12 Mintern, J. D., Guillonnet, C., Carbone, F. R., Doherty, P. C. and Turner, S. J., Cutting edge: tissue-resident memory CTL down-regulate cytolytic molecule expression following virus clearance. *J. Immunol.* 2007. **179**: 7220–7224.
- 13 Best, S. M., Viral subversion of apoptotic enzymes: escape from death row. *Annu. Rev. Microbiol.* 2008. **62**: 171–192.
- 14 Lieberman, J. and Fan, Z., Nuclear war: the granzyme A-bomb. *Curr. Opin. Immunol.* 2003. **15**: 553–559.
- 15 Mullbacher, A., Ebnet, K., Blanden, R. V., Hla, R. T., Stehle, T., Museteanu, C. and Simon, M. M., Granzyme A is critical for recovery of mice from infection with the natural cytopathic viral pathogen, ectromelia. *Proc. Natl. Acad. Sci. USA* 1996. **93**: 5783–5787.
- 16 Metkar, S. S., Mena, C., Pardo, J., Wang, B., Wallich, R., Freudenberg, M., Kim, S. et al., Human and mouse granzyme A induce a proinflammatory cytokine response. *Immunity* 2008. **29**: 720–733.
- 17 Johnson, B. J., Costelloe, E. O., Fitzpatrick, D. R., Haanen, J. B., Schumacher, T. N., Brown, L. E. and Kelso, A., Single-cell perforin and granzyme expression reveals the anatomical localization of effector CD8<sup>+</sup> T cells in influenza virus-infected mice. *Proc. Natl. Acad. Sci. USA* 2003. **100**: 2657–2662.
- 18 Peixoto, A., Evaristo, C., Munitic, I., Monteiro, M., Charbit, A., Rocha, B. and Veiga-Fernandes, H., CD8 single-cell gene coexpression reveals three different effector types present at distinct phases of the immune response. *J. Exp. Med.* 2007. **204**: 1193–1205.
- 19 Takata, H. and Takiguchi, M., Three memory subsets of human CD8<sup>+</sup> T cells differently expressing three cytolytic effector molecules. *J. Immunol.* 2006. **177**: 4330–4340.
- 20 Rock, M. T., Yoder, S. M., Wright, P. F., Talbot, T. R., Edwards, K. M. and Crowe, J. E., Jr., Differential regulation of granzyme and perforin in effector and memory T cells following smallpox immunization. *J. Immunol.* 2005. **174**: 3757–3764.
- 21 Grossman, W. J., Verbsky, J. W., Tollefsen, B. L., Kemper, C., Atkinson, J. P. and Ley, T. J., Differential expression of granzymes A and B in human cytotoxic lymphocyte subsets and T regulatory cells. *Blood* 2004. **104**: 2840–2848.
- 22 Fehniger, T. A., Cai, S. F., Cao, X., Bredemeyer, A. J., Presti, R. M., French, A. R. and Ley, T. J., Acquisition of murine NK cell cytotoxicity requires the translation of a pre-existing pool of granzyme B and perforin mRNAs. *Immunity* 2007. **26**: 798–811.
- 23 Masopust, D., Vezys, V., Marzo, A. L. and Lefrancois, L., Preferential localization of effector memory cells in nonlymphoid tissue. *Science* 2001. **291**: 2413–2417.
- 24 Wallace, M. E., Keating, R., Heath, W. R. and Carbone, F. R., The cytotoxic T-cell response to herpes simplex virus type 1 infection of C57BL/6 mice is almost entirely directed against a single immunodominant determinant. *J. Virol.* 1999. **73**: 7619–7626.
- 25 Kelso, A., Costelloe, E. O., Johnson, B. J., Groves, P., Buttigieg, K. and Fitzpatrick, D. R., The genes for perforin, granzymes A–C and IFN- $\gamma$  are differentially expressed in single CD8(+) T cells during primary activation. *Int. Immunol.* 2002. **14**: 605–613.
- 26 Bell, J. K., Goetz, D. H., Mahrus, S., Harris, J. L., Fletterick, R. J. and Craik, C. S., The oligomeric structure of human granzyme A is a determinant of its extended substrate specificity. *Nat. Struct. Biol.* 2003. **10**: 527–534.
- 27 Kaiserman, D., Bird, C. H., Sun, J., Matthews, A., Ung, K., Whisstock, J. C., Thompson, P. E. et al., The major human and mouse granzymes are structurally and functionally divergent. *J. Cell Biol.* 2006. **175**: 619–630.
- 28 Cullen, S. P., Adrain, C., Luthi, A. U., Duriez, P. J. and Martin, S. J., Human and murine granzyme B exhibit divergent substrate preferences. *J. Cell Biol.* 2007. **176**: 435–444.
- 29 La Gruta, N. L., Turner, S. J. and Doherty, P. C., Hierarchies in cytokine expression profiles for acute and resolving influenza virus-specific CD8<sup>+</sup> T cell responses: correlation of cytokine profile and TCR avidity. *J. Immunol.* 2004. **172**: 5553–5560.
- 30 La Gruta, N. L., Doherty, P. C. and Turner, S. J., A correlation between function and selected measures of T cell avidity in influenza virus-specific CD8<sup>+</sup> T cell responses. *Eur. J. Immunol.* 2006. **36**: 2951–2959.
- 31 Belz, G. T., Xie, W. and Doherty, P. C., Diversity of epitope and cytokine profiles for primary and secondary influenza A virus-specific CD8<sup>+</sup> T cell responses. *J. Immunol.* 2001. **166**: 4627–4633.

- 32 Nakajima, H., Park, H. L. and Henkart, P. A., Synergistic roles of granzymes A and B in mediating target cell death by rat basophilic leukemia mast cell tumors also expressing cytolysin/perforin. *J. Exp. Med.* 1995. **181**: 1037–1046.
- 33 La Gruta, N. L., Kedzierska, K., Stambas, J. and Doherty, P. C., A question of self-preservation: immunopathology in influenza virus infection. *Immunol. Cell Biol.* 2007. **85**: 85–92.
- 34 Jenkins, M. R., Trapani, J. A., Doherty, P. C. and Turner, S. J., Granzyme K expressing cytotoxic T lymphocytes protects against influenza virus in granzyme AB<sup>-/-</sup> mice. *Viral Immunol.* 2008. **21**: 341–346.
- 35 Jenkins, M. R., Webby, R., Doherty, P. C. and Turner, S. J., Addition of a prominent epitope affects influenza A virus-specific CD8<sup>+</sup> T cell immunodominance hierarchies when antigen is limiting. *J. Immunol.* 2006. **177**: 2917–2925.
- 36 Hogquist, K. A., Jameson, S. C., Heath, W. R., Howard, J. L., Bevan, M. J. and Carbone, F. R., T cell receptor antagonist peptides induce positive selection. *Cell* 1994. **76**: 17–27.

**Abbreviations:** D<sup>b</sup>NP<sub>366</sub>: H-2D<sup>b</sup> + nucleoprotein amino acid residues 366–374 · D<sup>b</sup>PA<sub>224</sub>: H-2D<sup>b</sup> + acid polymerase amino acids 224–233 · D<sup>b</sup>F2<sub>62</sub>: H-2D<sup>b</sup> + alternative reading frame polymerase B amino acids 62–70 · grz: granzyme · K<sup>b</sup>PB1<sub>703</sub>: H-2K<sup>b</sup> + polymerase B amino acids 703–711 · K<sup>b</sup>gB<sub>498</sub>: H-2K<sup>b</sup> + glycoprotein B amino acid residues 498–505 · KLRG-1: killer cell lectin-like receptor G-1 · K<sup>b</sup>NS2<sub>114</sub>: H-2K<sup>b</sup> + non-structural protein 2 NS2 amino acids 114–121 · K<sup>b</sup>OVA<sub>257</sub>: H-2K<sup>b</sup> + OVA amino acid residues 257–264 · MLN: mediastinal LN · pfp: perforin · X31: A/HKx31

**Full correspondence:** Dr. Stephen J. Turner, Department of Microbiology and Immunology, The University of Melbourne, Parkville, Victoria 3010, Australia

Fax: +61-3-93471540

e-mail: sjturn@unimelb.edu.au

Received: 17/12/2008

Revised: 2/2/2009

Accepted: 26/2/2009